Appl Nanosci (2013) 3:153–159
DOI 10.1007/s13204-012-0089-5

ORIGINAL ARTICLE

Optical and magnetic properties of $Zn_{0.98}Mn_{0.02}O$ nanoparticles

Talaat M. Hammad · S. Griesing · M. Wotocek · S. Kuhn · R. Hempelmann · U. Hartmann · Jamil K. Salem

Received: 21 February 2012 / Accepted: 7 March 2012 / Published online: 25 March 2012

Abstract Pure and Mn-doped colloidal ZnO particles were prepared in a solvo-thermal via sol–gel process by base-catalyzed hydrolysis of zinc acetate. We have studied the structural, magnetic and optical properties of the samples using X-ray diffraction (XRD), transmission electron microscopy, energy dispersive X-ray analysis, superconducting quantum interferometer device and UV–Vis spectroscopy. The XRD spectra show that all the samples are hexagonal wurtzite structures. The calculated average particle size of the samples was approximately 7–3 nm, indicating that the particle size decreased by doping with manganese. Magnetic investigations showed that at room temperature the Mn-doped ZnO possessed ferromagnetism with the saturation magnetic moment of 0.194 emu/g. The room temperature PL measurements illustrate UV-emission centered at 351 nm (3.53 eV), which is ascribed to the near-band-edge emissions of ZnO, violet emission at 512 nm (2.42 eV). The UV–Vis spectra showed a blue-shift from 3.42 to 3.78 eV when the ZnO doped with manganese.

T. M. Hammad (✉)
Department of Physics, Al-Azhar University,
P. O. Box 1244, Gaza, Palestine
e-mail: talaat@yahoo.com

S. Griesing · U. Hartmann
Department of Experimental Physics, Saarland University,
66123 Saarbrucken, Germany

M. Wotocek · S. Kuhn · R. Hempelmann
Department of Physical Chemistry,
Saarland University, 66123 Saarbrucken, Germany

J. K. Salem
Department of Chemistry, Al-Azhar University,
P. O. Box 1244, Gaza, Palestine

Keywords Structural · Optical · Magnetic · Mn-doped ZnO · Nanoparticles

Introduction

Oxide-based dilute magnetic semiconductors (DMS) have attracted considerable attention because of the possibility of incorporating ferromagnetism in a semiconducting oxide. The metal oxide, ZnO, a wideband-gap semiconductor with a large exciton binding energy of 60 meV at room temperature, is an exceptionally important material for the envisaged applications in many technologies, such as solar energy conversion and optoelectronic devices (Hammad et al. 2010). Of late, much experimental and theoretical research is focused on DMS based on transition metals (TM), such as Mn, Ni and Co-doped ZnO, because of their expected potential applications in future spintronics (Bauer et al. 2001). Interestingly in these systems, the origin of ferromagnetism remains an issue of debate, and there is a great deal of controversy over the origin of ferromagnetism. Room temperature ferromagnetism (Sharma et al. 2003; Cong et al. 2005; Schwartz et al. 2004; Radovanovic and Gamelin 2003; Barick and Bahadur 2007; Wang et al. 2007) is observed in several TM-doped ZnO materials. There are also reports of ferromagnetism only at low temperature (Jung et al. 2002; Wakano et al. 2001) spin glass (Fukamura et al. 2001), and paramagnetic (Kolesnik et al. 2004; Rao and Deepak 2005; Yin et al. 2005; Clavel et al. 2007) behavior in these systems. While the controversy is obvious, the properties seem to be a strong function of the conditions of preparation. Furthermore, most of the previous investigations have focused on thin films and bulk, and there are much less reports on

nanoparticles of transition metal-doped ZnO. Studies have been carried out to fine-tune the properties of ZnO to adopt it for different applications; for e.g., the band gap of ZnO is modified to use as UV detectors and emitters (Tang et al. 1998). Doping Mn into the bulk ZnO matrix offers an interesting way to alter various properties (Fukamura et al. 1999), for example, the band gap of the host material can be tuned from 3.3 to 3.7 eV. In addition, it also alters the emission properties by providing an efficient channel for the recombination of the electron and the hole via the dopant Mn d levels. The optical and electronic properties of semiconductors can be further tuned by varying the size of the particles in the range below 10 nm. In addition, it is recently reported (Sharma et al. 2009) that Mn-doped ZnO thin films as well as in bulk exhibit ferromagnetism at room temperature. Studies on various Mn-doped semiconductor nanocrystals (Levy et al. 1996) have revealed that the properties of these samples, like the band gap, are influenced by the quantum confinement of electronic states; accordingly, these properties of the doped nanocrystals are considerably different compared to those of the doped bulk system (Sapra et al. 2002). These interesting changes in confined DMSs have enlarged the scope of research activity in this field, prompting us to study the confinement effects in Mn-doped ZnO nanocrystals.

The aim of this work is to evaluate the effect of Mn doping on the microstructure, magnetic and the optical properties of the powder grown by simple solvo-thermal method. In this letter, we report the changes in the optical properties of ZnO nanocrystals brought about by successful doping with Mn ions.

Experiment procedure

The dispersed ZnO nanoparticles were prepared according to the route described in Spanhel and Anderson (1991). In our case, the synthesis was carried out under ambient-temperature conditions. Typically 9.8 mmol $Zn(OAC)_2{\cdot}2H_2O$ and 0.2 mmol $Mn(OAC)_2{\cdot}4H_2O$ were dissolved at 70 °C in 200 mL ethanol under stirring, subsequently cooled to 50 °C. In a second flask, 5.0 mmol $LiOH{\cdot}H_2O$ were dissolved under ultra sound in 200 mL ethanol (Dong et al. 2005). $LiOH{\cdot}H_2O$ dissolved in ethanol was added dropwise under stirring during 1 h to the Zn Mn acetate solution. The product was stirred for another hour at 50 °C and cooled down to room temperature. After that the solution was absolutely clear. 800 mL *n*-hexane were added to precipitate the doped ZnO. Then, the precipitate of doped ZnO was separated by centrifuging at 4,500 rpm for 1 h. The obtained precipitate was washed twice with 100 mL ethanol, 300 mL *n*-hexane and centrifuged at 4,500 rpm for 3 h, and then drying at 60 °C for 3 h.

The UV absorption spectra were taken with a Hewlett Packard8453 spectrometer. The fluorescence measurements were done with a Perkin–Elmer LS 50B luminescence spectrometer. The transmission electron microscopy (TEM) analysis was done with a Tecnai F300 transmission electron microscope, images taken after suspending in 95 % ethanol. Crystal structure identification and crystal size analysis were carried out by X-ray diffraction (XRD) XDS 2000, Scintac Inc., USA with CuKα radiation source, and scan rate of 2°/min. The morphology of the film is characterized by atomic force microscopy (AFM). Magnetic characterization was carried out using a superconducting quantum interferometer device (SQUID), Quantum Design MPMS XL-7 magnetometer in RSO mode.

Results and discussion

Powder XRD patterns of undoped ZnO and Mn-doped ZnO nanoparticles are shown in Fig. 1. The diffraction peaks in Fig. 1 could readily indexed the hexagonal phase of ZnO, the lattice parameters of which were all consistent with the reported values (JPCDS-1451). It is evident from the XRD data that there are no extra peaks due to manganese metal, other oxides or any zinc manganese phase, indicating that the as-synthesized samples are single phase. The Mn ion was understood to have substituted the Zn site without changing the wurtzite structure. The Debye–Scherrer equation gives the relation between the mean particle size and the full-width of a peak at half-maximum (FWHM) in a polycrystalline sample; it can be expressed as

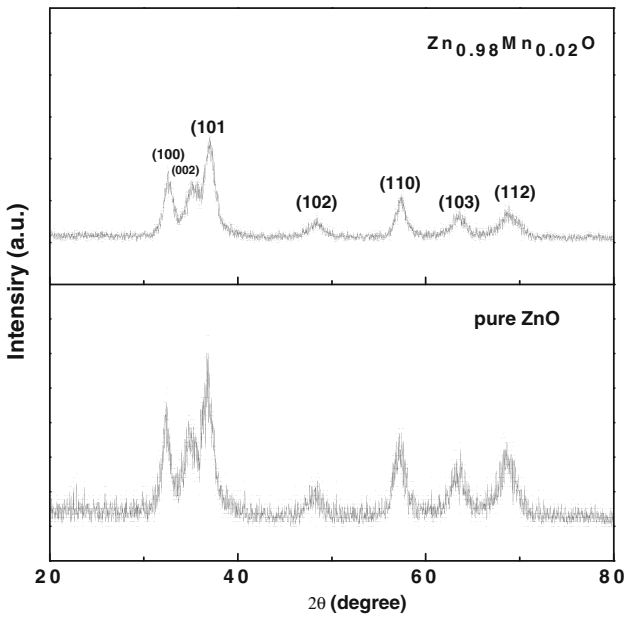

Fig. 1 X-ray diffraction patterns of pure and $Zn_{0.98}Mn_{0.02}O$ nanoparticles

$$d = \frac{0.89\lambda}{(\beta \cos\theta)}$$

where d, λ, θ and β denote the mean grain size, the X-ray wavelength (1.5406 Å), the Bragg diffraction angle, and the FWHM, respectively. The calculated average particle size of the samples was approximately 3 and 7 nm, with smaller particle size values for the samples doped with manganese. This may be due to the ionic radius of Mn^{2+} (0.83 Å) that is larger than the ionic radius of Zn^{2+} (0.74 Å).

The morphology of Mn-doped ZnO nanoparticles was investigated by high-resolution TEM. Figure 2 shows the TEM images of pure and $Zn_{0.98}Mn_{0.02}O$ nanoparticles. TEM images of samples were uniform with well-distributed spherical or elliptical particles with a particle size between 3 and 7 nm. This result strongly suggested that Mn atoms were incorporated uniformly into the entire material and no segregated metal impurity phase appeared. This is consistent with estimated particle size from the XRD peak broadening. The result of HRTEM characterizations are shown in Fig. 3a and b. From HRTEM images, it is clearly observed that the average particle size of $Zn_{0.98}Mn_{0.02}O$ nanoparticles was about 3 nm, which is consistent with the calculation results from XRD. It is also clear from HRTEM results that Mn doping in ZnO reduces the particle size. The average interfringe distance of $Zn_{0.98}Mn_{0.02}O$ nanoparticles was measured to be

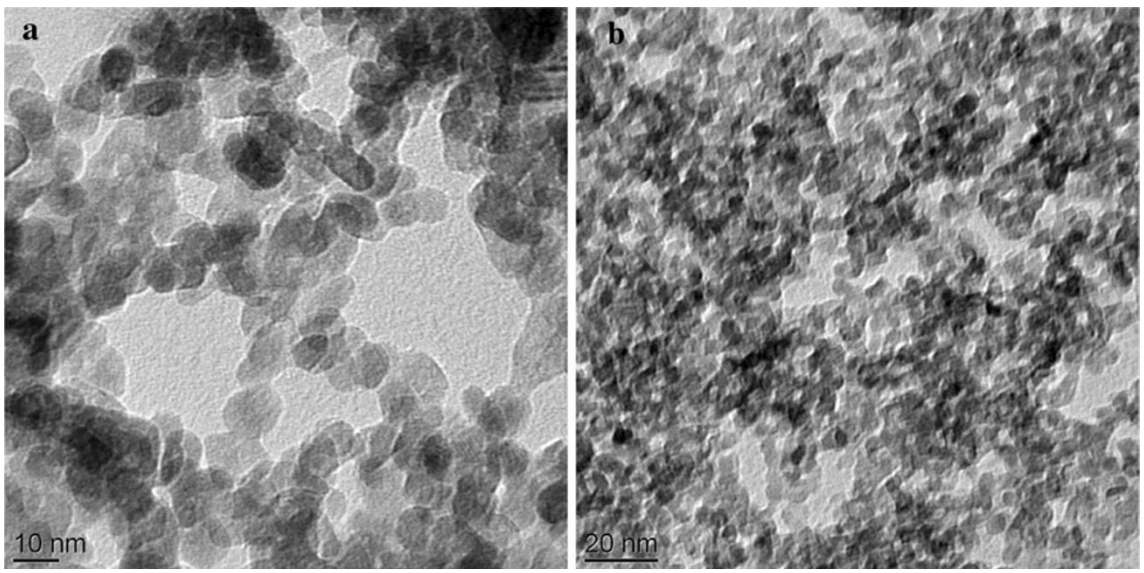

Fig. 2 TEM micrographs of pure and Mn-doped ZnO: **a** pure ZnO and **b** $Zn_{0.98}Mn_{0.02}O$ nanoparticles

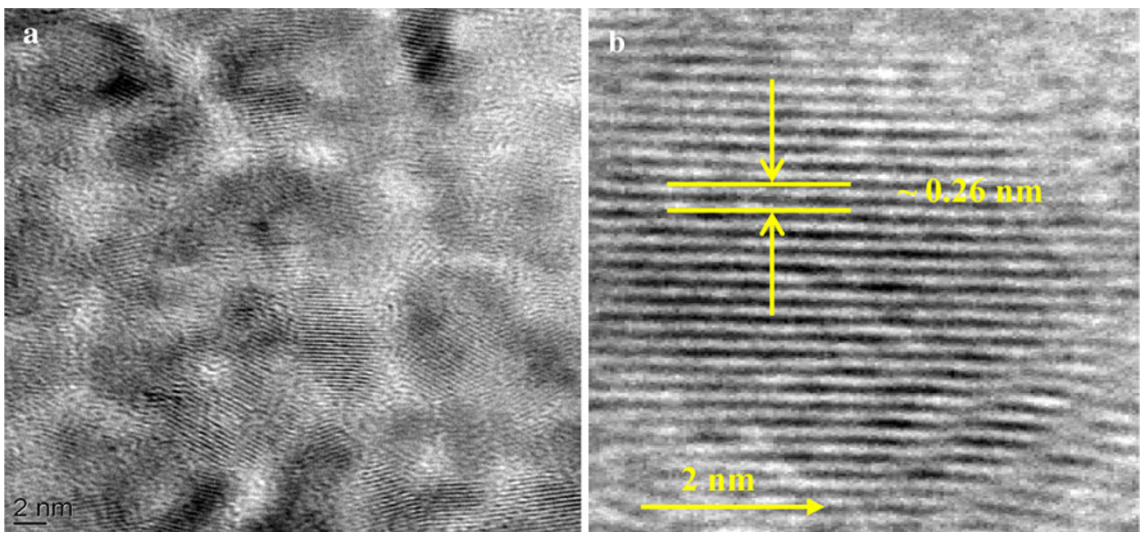

Fig. 3 **a**, **b** HRTEM images of $Zn_{0.98}Mn_{0.02}O$ nanoparticles

~0.26 nm. According to the results of XRD pattern and HRTEM images, we believed that the Mn ions were well incorporated into the crystal lattice of ZnO. The EDX analysis of Mn-doped ZnO and $Zn_{0.98}Mn_{0.02}O$ nanoparticles is shown in Fig. 4. The EDX spectrum confirms the presence of manganese in the ZnO particles and observed atomic percentage (%) is close to the nominal value of Mn in ZnO. Table 1 lists the atomic percentages of the elements present in the Mn-doped ZnO sample.

The effect of Mn doping on the band gap of ZnO and substitution of Mn^{2+} ions in tetrahedral sites of wurtzite structure ZnO was further confirmed using UV–Vis optical spectroscopy measured at room temperature. Figure 5 shows the UV-absorption spectra of pure ZnO and Mn-doped ZnO nanoparticles. The absorption band edge of pure ZnO is observed at 363 nm and corresponds to a band gap of 3.42 eV, indicating a blue shift of about 0.36 eV as compared to the band gap of Mn-doped ZnO of 3.78 eV (328 nm). Many other researchers (Rusu et al. 2010; Srinivasan and Kumar 2008; Fukamura et al. 2001; Chikoidze et al. 2007; Wang et al. 2006) reported the blue shift of the fundamental absorption edge with the increase of the Mn content in the doped ZnO films and the presence of an additional absorption band in front of the absorption edge. This optical behavior is attributed mainly to the sp–d spin exchange interaction between the band electrons and the localized d electrons of Mn^{+2} ions.

Room temperature photoluminescence (PL) spectra of pure ZnO and Mn-doped ZnO samples were measured using photoluminescence spectroscopy. Figure 6 shows the PL spectra of pure ZnO and of $Zn_{0.98}Mn_{0.02}O$ at an excitation wavelength of 320 nm. The PL spectra (Fig. 6) consist of two UV emission peaks which centered at 351 nm (3.53 eV) and 342 nm (3.61 eV), respectively, and a broad green emission band centered at 512 nm (2.42 eV). With manganese doped into the ZnO crystal lattice, the intensity of the peaks for the UV and green emission is reduced. Mn doping is expected to cause an reduction in the intensity of both UV (Hammad et al. 2009) and green emission (Hammad et al. 2009; Salem et al. 2009). It can be found that the optical band gap is increased when Mn

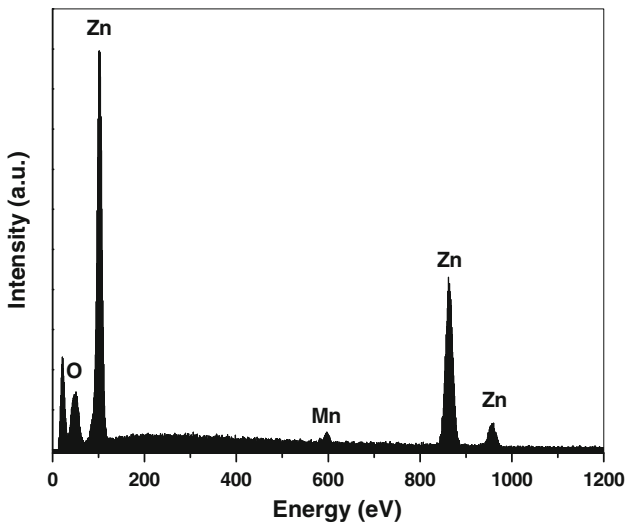

Fig. 4 EDX spectrum of $Zn_{0.98}Mn_{0.02}O$ nanoparticles

Table 1 The atomic percentage calculated for $Zn_{0.98}Mn_{0.02}O$ nanoparticles

Element	Atomic percentage (%)
Mn	1.47 ± 0.33
Zn	48.06 ± 0.38

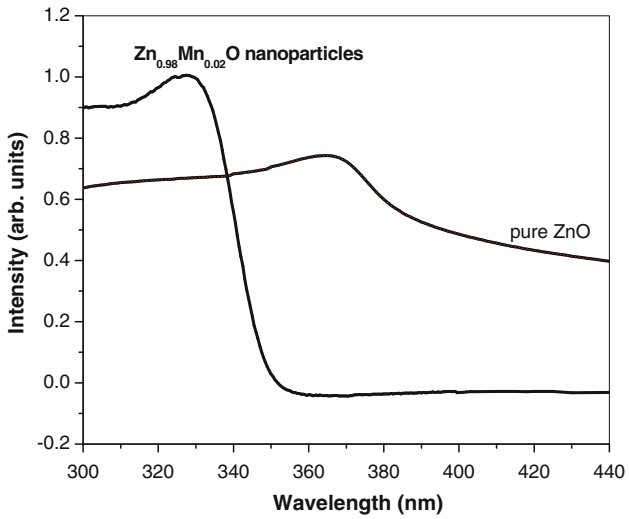

Fig. 5 UV–Vis spectra of pure and $Zn_{0.98}Mn_{0.02}O$ nanoparticles

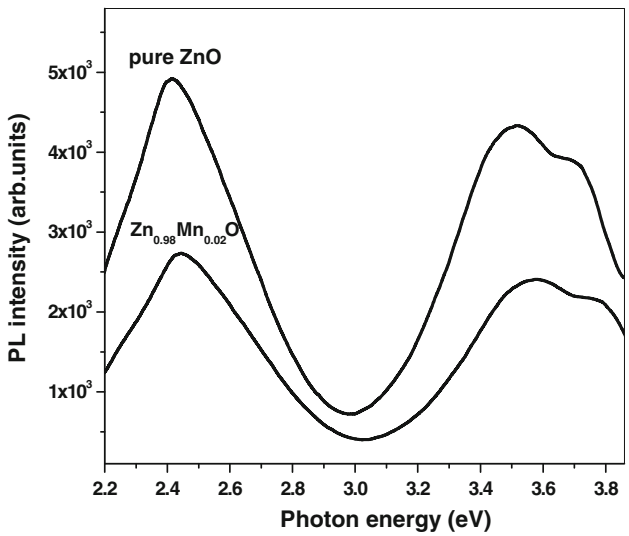

Fig. 6 PL spectra of pure and $Zn_{0.98}Mn_{0.02}O$ nanoparticles

was doped in ZnO nanoparticles. Since the band gap of MnO (bulk value 4.2 eV) is higher than that ZnO (bulk value 3.32 eV), the band gap of Mn-doped ZnO should be larger than the band gap of ZnO. A similar observation of enhancement of the band gap of ZnO with Mn was also made by Fukumura et al. (2001) and Yan et al. (2011). It is commonly considered that UV emission of the wide band gap ZnO semiconductor attributed to exciton transitions from localized levels is below the conduction band to the valence band (Wang et al. 2006; Huang et al. 2001; Cho et al. 2002; Zu et al. 1997). The localized level assumed to originate from the free impurity atoms and various defects related to oxygen and zinc. Moreover, the origin of the defect-related visible emission in ZnO nanomaterials may be ascribed to the oxygen vacancies and the intrinsic defects (Li et al. 2006; Sun et al. 2006). The green emission observed in the visible region may be attributed to the impurity levels correspond to the singly ionized oxygen vacancy in ZnO (Monticone et al. 1998a, b).

To study how the concentration of Mn atom changes the magnetic behavior of our Mn-doped ZnO nanoparticles, a magnetization (M) versus applied field (H) study was performed at room temperature using superconducting quantum interferometer. Figure 7 shows the magnetic hysteresis (M–H) curves of pure ZnO and $Zn_{0.98}Mn_{0.02}O$ nanoparticles measured at room temperature. The hysteresis loop reveals that the saturation magnetization Ms and the coercivity Hc of pure and doped ZnO nanoparticles are about 0.014 emu/g, 4.3 Oe, 00.194 emu/g and 272 Oe, respectively. Furthermore, the doped ZnO sample exhibits higher magnetization values than that of the pure ZnO sample. This magnetization of present doped ZnO is larger

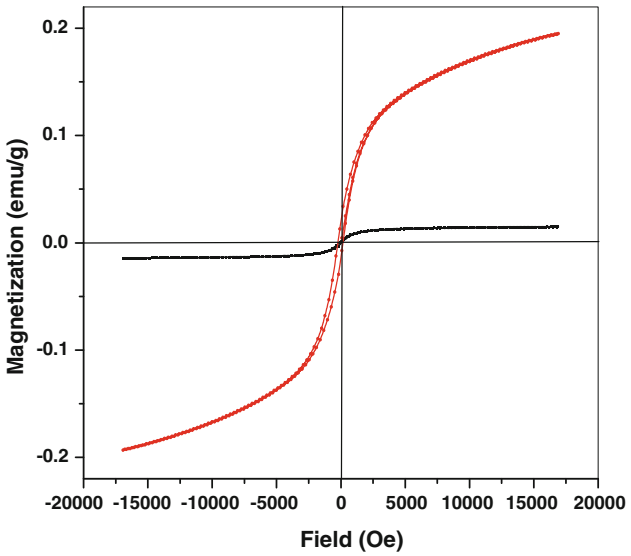

Fig. 7 Magnetization of Mn-doped ZnO nanoparticle as a function of field measured at room temperature

than values were reported by Jayakumar et al. 2007 and Ma and Lou1 (2011). Jayakumar et al. 2007 have observed that the value of magnetization of 2.5 % Mn-doped ZnO nanoparticles at room temperature is 0.034 emu/g.

However, Ma and Lou1 (2011) estimated the magnetization of 10 % Mn-doped ZnO nanoparticles to be 0.015 emu/g.

Ferromagnetism in dilute magnetic semiconductors is considered to originate from the exchange interaction between free delocalized carriers (holes or electrons from the valence band) and the localized d spins on the TM ions (Dietl et al. 2000). Therefore, the presence of free carriers and localized d spins is a prerequisite for the appearance of ferromagnetism. These defects like Zn interstitials and O vacancies usually induce *n*-type characteristics. The mechanism for intrinsic ferromagnetism in $Zn_{1-x}Mn_xO$ thin films still remains unclear, and the source of ferromagnetism remains controversial. However, detailed structural characterization minimizes the possibility that the ferromagnetism is due to any impurity phases in our samples. It has been proposed that uncontrolled formation of lattice defects can generate carriers that mediate ferromagnetic behavior (Venkatesan et al. 2004; Coey et al. 2005). Recently, Sundaresan et al. (2006) observed that metal oxides such as CeO_2, Al_2O_3, ZnO, In_2O_3 and SnO_2 in nanoparticulate form exhibit room temperature ferromagnetism presumably due to the exchange interaction between localized spin moments resulting from the oxygen vacancies at the surface of nanoparticles. The native point defects such as oxygen vacancies are very common in ZnO nanoparticles giving rise to ferromagnetic behavior. Interestingly, as compared to single nanoparticles, these self-aggregated ZnO superstructure exhibits an higher magnetization, which may be due to the formation of higher amount of defects as a result of oriented attachment among nanocrystals. In comparison to pure ZnO superstructures, Mn and Ni doping may increase the concentration of oxygen vacancy because of their slightly larger ionic radii than Zn ions.

Conclusion

Manganese-doped ZnO nanoparticles have been successfully prepared in a sol–gel process by base-catalyzed hydrolysis of zinc acetate. Microstructure analysis confirms the single phase hexagonal wurtzite structure for Mn-doped ZnO and spherical nanoparticles were observed through TEM images. The average particle size calculated from XRD patterns of the samples was approximately 7–3 nm, indicating that the particle size decreased by doping with manganese. Magnetic investigations showed that the Mn-doped ZnO nanoparticles possessed room temperature

ferromagnetism with the saturation magnetic moment of 0.1 emu/g. The room temperature PL spectrum of the $Zn_{0.98}Mn_{0.02}O$ nanoparticles consisted of a strong UV NBE emission band at 351 nm and a broad green emission at around 530 nm. The UV NBE emission of the $Zn_{0.98}Mn_{0.02}O$ nanoparticles showed a blue shift owing to Mn substitution.

Acknowledgments The authors would like to gratefully appreciate the financial support from the DAAD and Saarland University, Germany.

References

Barick KC, Bahadur DJ (2007) Synthesis, self-assembly, and properties of Mn doped ZnO nanoparticles. J Nanosci Nanotechnol 7:1935–1940

Bauer C, Boschloo G, Mukhtar E, Hagfeldt A (2001) Electron injection and recombination in $Ru(dcbpy)_2(NCS)_2$ sensitized nanostructured ZnO. A J Phys Chem B 105:5585–5588

Chikoidze E, Dumont Y, Jomard F, Gorochov O (2007) Electrical and optical properties of ZnO:Mn thin films grown by MOCVD. Thin Solis Films 515:8519–8523

Cho YM, Choo WK, Kim H, Kim D, Ihm YE (2002) Effects of rapid thermal annealing on the ferromagnetic properties of sputtered $Zn_{1-x}(Co_{0.5}Fe_{0.5})_xO$ thin films. Appl Phys Lett 80:3358–3360

Clavel G, Willinger M-G, Zitoun D, Pinna N (2007) Solvent dependent shape and magnetic properties of doped ZnO nanostructures. Adv Funct Mater 17:3159–3169

Coey JMD, Venkatesan M, Fitzgerald CB (2005) Donor impurity band exchange in dilute ferromagnetic oxides. Nat Mater 4:173–179

Cong CJ, Liao L, Li JC, Fan LX, Zhang KL (2005) Synthesis, structure and ferromagnetic properties of Mn-doped ZnO nanoparticles. Nanotechnol 16:981–984

Dietl T, Ohno H, Matsukura F, Cibert J, Ferrand D (2000) Zener model description of ferromagnetism in zinc-blende magnetic semiconductors. Science 287:1019–1022

Dong L, Liu YC, Tong YH, Xiao ZY, Zhang JY, Lu YM, Shen DZ, Fan XW (2005) Preparation of ZnO colloids by aggregation of the nanocrystal subunits. J Colloid Interface Sci 15:380–384

Fukamura T, Jin Z, Ohtomo A, Koinuma H, Kawasaki M (1999) An oxide-diluted magnetic semiconductor: Mn-doped ZnO. Appl Phys Lett 75:3366–3369

Fukamura T, Jin Z, Kawasaki M, Shono T, Hasegawa T, Koshihara S, Koinuma H (2001) Magnetic properties of Mn-doped ZnO. Appl Phys Lett 78:958–961

Hammad T, Salem JK, Harrison RG (2009) Synthesis, characterization, and optical properties of Y-doped ZnOnanoparticles. NANO 4:225–232

Hammad T, Salem JK, Harrison RG (2010) The influence of annealing temperature on the structure, morphologies and optical properties of ZnO nanoparticles. Superlattices Microstruct 47:335–340

Huang MH, Wu YY, Feick HN, Tran N, Weber E, Yang PD (2001) Room-temperature ultraviolet nanowire nanolasers. Adv Mater 13:113

Jayakumar OD, Gopalakrishnan IK, Kadam RM, Vinu A, Asthana A, Tyagi AK (2007) Magnetization and structural studies of Mn doped ZnO nanoparticles: prepared by reverse micelle method. J Cryst Growth 300:358–363

Jung SW, An S-J, Yi G-C, Jung CU, Lee S-I, Cho S (2002) Ferromagnetic properties of $Zn_{1-x}Mn_xO$ epitaxial thin films. Appl Phys Lett 80:4561–4564

Kolesnik S, Dabrowski B, Mais J (2004) Structural and magnetic properties of transition metal substituted ZnO. J Appl Phys 95:2582–2587

Levy L, Hochepied JF, Pileni MP (1996) Control of the size and composition of three dimensionally diluted magnetic semiconductor clusters. J Phys Chem 100:18322–18326

Li C, Fang G, Fu Q, Su F, Li G, Wu XZ, Zhao X (2006) Effect of substrate temperature on the growth and photoluminescence properties of vertically aligned ZnO nanostructures. J Cryst Growth 292:19–25

Ma X, Lou C (2011) The dilute magnetic and optical properties of Mn-doped ZnO nanowires. J Nanomaterial 2011:464538–464543

Monticone S, Tufeu R, Kanaev AV (1998a) Complex nature of the UV and visible fluorescence of colloidal ZnO nanoparticles. J Phys Chem B 102:2854–2862

Monticone S, Tufeu R, Kanaev AV (1998b) Prepared in the presence of additives by thermal decomposition. Int J Nanosci 8:465–472

Radovanovic PV, Gamelin DR (2003) High temperature ferromagnetism in nanocrystalline Ni^{2+}-doped ZnO. Phys Rev Lett 92:157202

Rao CNR, Deepak FL (2005) Absence of ferromagnetism in Mn- and Co-doped ZnO. J Mater Chem 15:573–578

Rusu GG, Gorley P, Baban PC, Rambu AP, Rusu M (2010) Preparation and characterization of Mn-doped ZnO thin films. J Optoelectron Adv Mater 12:895–899

Salem JK, Hammad TM, Harrison RG (2009) ZnO nanoparticles prepared in the presence of additives by thermal decomposition. Int J Nanosci 8:465–472

Sapra S, Sarma DD, Sanvito S, Hill N (2002) Influence of quantum confinement on the electronic and magnetic properties of (Ga, Mn)As diluted magnetic semiconductor. A Nano Lett 2:605–608

Schwartz DA, Kittilstved KR, Gamelin DR (2004) Above room-temperature ferromagnetic Ni^{2+}-doped ZnO thin films prepared from colloidal diluted magnetic semiconductor quantum dots. Appl Phys Lett 85:1395–1398

Sharma P, Gupta A, Rao KV, Owens FJ, Sharma R, Ahuja R, Guillen JMO, Johansson B, Gehring GA (2003) Ferromagnetism above room temperature in bulk and transparent thin films of Mn-doped ZnO. Nat Mater 2:673–677

Sharma PK, Dutta RK, Pandey AC, Layek S, Verma HC (2009) Effect of iron doping concentration on magnetic properties of ZnO nanoparticles. J Magn Magn Mater 321:2587–2591

Spanhel L, Anderson MA (1991) Semiconductor clusters in the sol–gel process: quantized aggregation, gelation, and crystal growth in concentrated zinc oxide colloids. J Am Chem Soc 113(8): 2826–2833

Srinivasan G, Kumar J (2008) Effect of Mn doping on the microstructures and optical properties of sol–gel derived ZnO thin film. J Crys Growth 310:1841–1846

Sun Y, Ndifor-Angwafor NG, Riley DJ, Ashfold MNR (2006) Synthesis and photoluminescence of ultra-thin ZnO nanowire. Chem Phys Lett 431:352

Sundaresan A, Bhargavi R, Rangarajan N, Siddesh U, Rao CNR (2006) Ferromagnetism as a universal feature of nanoparticles of the otherwise nonmagnetic oxides. Phys Rev B74:161306(R)

Tang ZK, Wong GKL, Yu P, Kawasaki M, Ohtomo A, Koinuma H, Segawa Y (1998) Blue light-emitting diode based on ZnO. Appl Phys Lett 72:3270

Venkatesan M, Fitzgerald CB, Lunney JG, Coey JMD (2004) Anisotropic ferromagnetism in substituted zinc oxide. Phys Rev Lett 93:177206–177210

Wakano T, Fujimura N, Abe N, Ashida A, Ito T (2001) Magnetic and magneto-transport properties of ZnO:Ni films. Physica C 10:160–164

Wang YS, Thomas PJ, Brien PO (2006) Optical properties of ZnO nanocrystals doped with Cd, Mg, Mn, and Fe ions. J Phys Chem B 110(43):21412–21415

Wang H, Chen Y, Wang HB, Zhang C, Yang FJ, Duan JX, Yang CP, Xu YM, Zhou MJ, Li Q (2007) High resolution transmission electron microscopy and Raman scattering studies of room temperature ferromagnetic Ni-doped ZnO nanocrystal. Appl Phys Lett 90(5):052505

Yan X, Hu D, Li H, Li L, Chong X, Wang Y (2011) Nanostructure and optical properties of M doped ZnO (M = Ni, Mn) thin films prepared by sol–gel process. Physica B Phys Condensed Matter 406:3956

Yin ZG, Chen N, Yang F, Chai SL, Zhong J, Qian HJ, Ibrahim K (2005) Structural, magnetic properties and photoemission study of Ni-doped ZnO. Solid State Commun 135:430–433

Zu P, Tang ZK, Wong GKL, Kawasaki M, Ohtomo A, Koinuma HY, Segawa Y (1997) Ultraviolet spontaneous and stimulated emissions from ZnO microcrystallite thin films at room temperature. Solid State Commun 103:456–463